

International Conference on Space Optics—ICSO 2012

Ajaccio, Corse

9–12 October 2012

Edited by Bruno Cugny, Errico Armandillo, and Nikos Karafolas



Interferometric surface characterization of laser mirrors with sub-nanometer reproducibility for satellite-to-satellite optical metrology

Harald Kögel

Martin Gohlke

Domenico Gerardi

Joep Pijnenburg

et al.



Interferometric Surface Characterisation of Laser Mirrors with Sub-Nanometer Reproducibility for Satellite-to-Satellite Optical Metrology

Harald Kögel*, Martin Gohlke*[†], Domenico Gerardi*, Joep Pijnenburg[‡],
Thilo Schuldt[§], Ulrich Johann*, Claus Braxmaier*^{¶||} and Dennis Weise*

*Astrium GmbH - Satellites, 88039 Friedrichshafen, Germany

[†]Humboldt University, Department of Physics, 12489 Berlin, Germany

[‡]TNO Opto Mechatronics, 2600 Delft, The Netherlands

[§]University of Applied Sciences Konstanz, Institute of Optical Systems, 78462 Konstanz, Germany

[¶]University of Bremen, ZARM Center of Applied Space Technology and Microgravity, 28359 Bremen, Germany

^{||}DLR German Aerospace Center, Institute of Space Systems, 28359 Bremen, Germany

Abstract—Path length errors caused by beamwalk over the surface topography of optical components can have a detrimental influence on the accuracy of highly sensitive translational metrology, that is of particular relevance for In-Field Pointing payload concepts, investigated for the LISA space mission. This paper presents the results of our experimental and theoretical investigations in surface induced path length errors with a detailed characterisation of their magnitudes.

I. INTRODUCTION

Actuated mirrors for beam steering can induce path length errors due to scanning of the laser beam over the surface of optical components in its path. In space missions with high precision satellite-to-satellite laser interferometry for gravitational wave detection (LISA [1] / NGO [2]) or geodesy (NGGM [3] / GRACE FO [4]), these path length errors may cause a dominant error in the performance of the measurement instrument.

The work presented in this paper was specifically motivated by an alternative payload concept with In-Field Pointing (IFP), as proposed by Astrium for the LISA space mission, see [5] and [6], whose interferometers require measurement accuracies of a few tens of a pm in the mHz range for detection of gravitational waves. The payload concept includes an actuated mirror in one of the telescope's pupil planes for beam tracking, shown in Figure 1, that will correct changes in the inter arm angle of the triangular satellite formation caused by their individual orbit dynamics. The permitted error caused by changes in path length due to an actuation of the mirror has therefore also to be within this required pm scale. In this context we investigated surface induced path length errors experimentally and in theory, using interferometric profilometry with a highly sensitive heterodyne interferometer to characterise their amplitudes. Some experimental investigations within the topic of interferometric profilometry has already been performed, see [7] and [8], but they were mainly intended for mirror surface measurements and not the topic of involved surface induced path length errors.

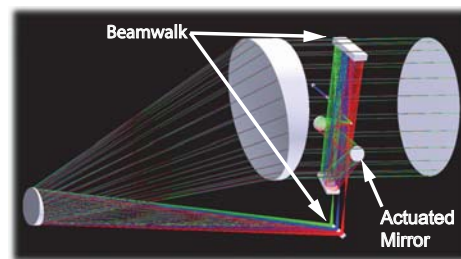


Fig. 1. Schematic of the LISA/NGO telescope for use within the alternative payload concept with In-Field Pointing. Marked are the actuated mirror for beam steering and the mirrors with the involved beamwalk.

II. MEASUREMENT SETUP

A test mirror with $\lambda/10$ surface figure is moved perpendicular to the outgoing measurement and reference laser beam of a highly sensitive heterodyne interferometer, that detects the surface induced phase changes as a translational signal. This interferometer uses a heterodyne frequency of 10 kHz and is housed in a vacuum chamber, see Figure 2 and [9]. The laser light is detected by two Quadrant Photo Detectors (QPDs) that additionally enable tilt measurements using the Differential Wavefront Sensing (DWS) technique. Data processing is performed by a digital, Field Programmable Gate Array (FPGA) based phasemeter, achieving measurement accuracies within few pm in translation and a few nrad in tilt.

The test mirror is supported in a special pendulum, shown in Figure 3, that enables highly reproducible movements due to a monolithic, clearance-free hinge and a high precision piezo walking actuator with a positioning accuracy of 5 nm. Parasitic movements, caused by manufacturing tolerances can be reduced by two adjustment mechanism, one for positioning the piezo actuator and one for positioning the point of driving force application on the pendulum.

The replaceable mirror support of the pendulum was designed for the accommodation of two test mirrors, which allows an

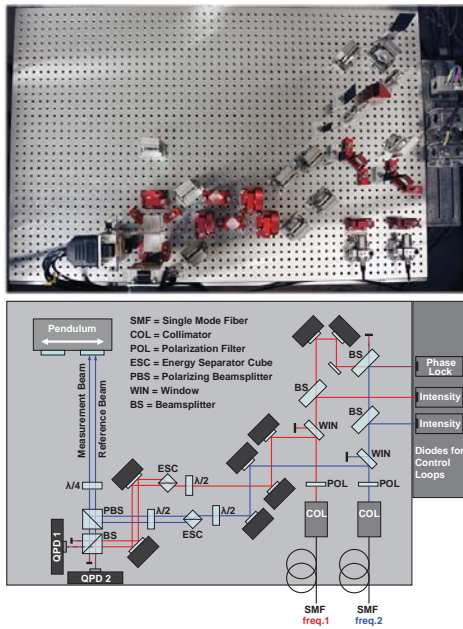


Fig. 2. Photograph of the heterodyne interferometer (top) and the schematic of its highly symmetric optical paths (bottom).

independent measurement with the measurement beam on the first and the reference beam on the second mirror to avoid correlation effects in the measurement results, caused by the manufacturing process of the mirror substrate. In this first investigations however, both laser beams are aligned onto one test mirror, schematically illustrated in Figure 4 [A], as the distance between them is only 4 mm. The laser beam diameters on the mirror surface were characterised by beam profiling with a razor blade of $\approx 1300 \mu\text{m}$.

III. MEASUREMENT PROCESS

During measurement the pendulum is moved in discrete steps of $10 \mu\text{m}$, which generates a quasi static condition between two steps, that is used for evaluation. On the one hand to avoid parasitic movements of the pendulum, caused by an inadequate guidance of the piezo actuator's runner and on the other hand to avoid the consideration of additional dynamic effects in the evaluation.

Common mode effects in the measured translation, resulting from e.g. parasitic movements of the pendulum or thermal expansions of the interferometer's breadboard, are suppressed by calculating the differential translation Δs between measurement and reference laser beam. As parasitic tilts of the pendulum result in translational measurement errors, the in-plane tilts α and the distance l between both laser beams are used for the correction of the differential translation, see equation 1. A typical correction is also shown in Figure 5.

$$\Delta s_{corr} = \Delta s \pm \tan\left(\frac{\alpha_{QPD1} + \alpha_{QPD2}}{2}\right) \cdot l \quad (1)$$

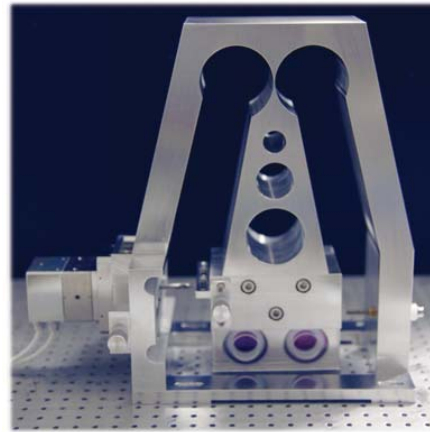


Fig. 3. Photograph of the pendulum with two test mirrors and the highly precise linear piezo actuator NEXLINE N-111.

IV. MEASUREMENT RESULTS

Typical measurement results are shown in Figure 6 (top). Amplitudes of the corrected differential translation in the range of some nanometers are observed, which is considerably larger than the required pm scale for LISA/NGO. The measured profiles are highly reproducible with a standard deviation σ from their mean value of 16 pm (best value) over measurement durations of 1500 s per run. Due to the identical laser beam diameters and beamwalk across the mirror surface of both laser beams, it is necessary to consider an additional amount of translation in the results, caused by the reference beam. Under assumption of statistically ideal topography the measured amplitudes should be over-estimated by a factor of $\sqrt{2}$ in the time domain.

To verify, that the observed signals indeed reflect the topography of the mirror surface and are not dominated by parasitic movements of the pendulum or other systematic errors, a simple test was performed. A tilted window was integrated into both laser beams, resulting in a lateral beam offset. The schematic of this setup is shown in Figure 4 [B]. Using Snell's law, the offset is theoretically calculated with $\approx 450 \mu\text{m}$, which should also be seen in the measurement results.

Figure 6 (middle) shows the results of the measurements with tilted window. A lateral offset of $\approx 460 \mu\text{m}$ with respect to the former measurement is existing, which implies that the measured profiles are mainly surface induced. Small differences in profile progression occur due to the circular movement of the test mirror and the involved slightly shifted measurement area, caused by the offset. After removing the tilted window, the same measurement results as in the initial measurement setup few days earlier were achieved, shown in Figure 6 (bottom).

As this measurement results show in general a limited lateral resolution due to the finite laser beam diameters, a lens with focal length 12 mm was put into the measurement laser beam, resulting in a reduced beam diameter of $\approx 13 \mu\text{m}$.

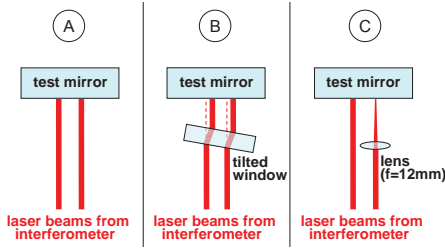


Fig. 4. Used measurement setups: [A] Initial setup; [B] Setup with tilted window for testing the influence of parasitic pendulum movements in the measurement results; [C] Setup with lens for an improved lateral resolution;

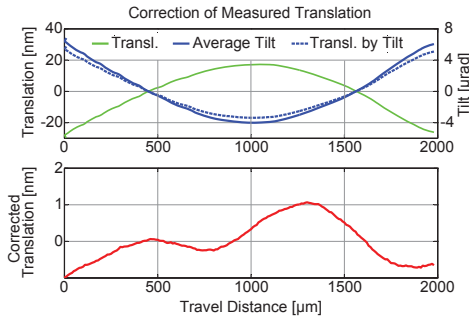


Fig. 5. Correction process for translational errors due to parasitic tilts of the pendulum during measurement.

This measurement setup is shown in Figure 4 [C]. A smaller laser beam diameter results in a reduced loss of surface information due to averaging the laser light on the QPDs, which increases the lateral resolution. The step size of the pendulum was adapted to the new laser beam diameter using now 2 µm, as smaller steps showed no further improvement.

With this new setup, measurement results with highly improved lateral resolutions were achieved, shown in Figure 7. The profiles have got higher amplitudes than in the former measurements without lens, and the reproducibility with a standard deviation σ from their mean value of 53 pm (best value) is slightly reduced. This is most likely attributed to the longer measurement durations of 7500 s per run, due to the slower driving velocity of the pendulum and the involved long time drift of the interferometer. As the in-plane tilt of the focussed measurement beam is observed to be subject to the local curvature of the mirror topography, only the tilt of the reference beam is used for the translational correction of the differential translation.

In order to independently validate these measurement results, comprehensive measurements were performed by the Physikalisch Technische Bundesanstalt (PTB) in Germany using interference microscopy with phase shifting for the surface measurements of a similar test mirror (same manufacturing batch as the test mirror used in the pendulum). Comparable results were achieved by multiplying the PTB measurement data z with a filter function f_{filter} that simulates the "low pass" filter effect for spatial frequencies of a Gaussian beam, see equation 2.

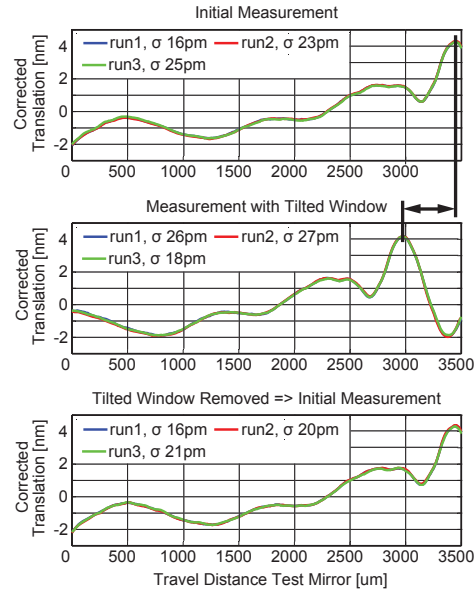


Fig. 6. Measurement results with unfocussed laser beams. Top: Initial measurement; Middle: Measurement with tilted window for excluding an influence of parasitic pendulum movements in the measurement results; Bottom: Measurement with removed tilted window → Initial measurement; The standard deviation σ for the different runs of each measurement are printed in the appendant legend.

$$z_{filter}(x_0, y_0) = \sum_{y=1}^n \sum_{x=1}^n z(x, y) \cdot f_{filter}(x, y, x_0, y_0) \quad (2)$$

With

$$f_{filter}(x, y, x_0, y_0) = \frac{2}{\pi \cdot r^2} \cdot e^{-2 \cdot \left(\frac{(x-x_0)^2 + (y-y_0)^2}{r^2} \right)} \quad (3)$$

The results after filtering show a smoothed topography. Depending on the used filter (for 1300 µm or 13 µm beam diameter), different spatial frequencies are cut off, consistent to the measurement results with the pendulum. As the measurement area of the interference microscopy is limited to 416 µm x 312 µm, a comparison using the Power Spectral Density (PSD) of the measured surface topography is only reasonable for the interferometric measurement results with focussed laser beam and the corresponding filtered PTB data.

To gain further insight a theoretical model of the pendulum measurements was developed. The problem of determining analytically path length errors resulting from a uniform (quasi-static) walk of a laser beam with finite-diameter over a mirror surface was considered. Building on the treatment in [10] and [11], an analytical model for the path length errors in several equivalent representations was derived. After that, the model for the characterization of the surface induced path length errors was applied. Key working assumptions and modeling equations are shortly summarized hereafter. To allow for a quick comparison in a PSD with the spectra derived from the measurements, results are expressed here in the spatial frequency domain f . The laser beam is modeled as a Gaussian

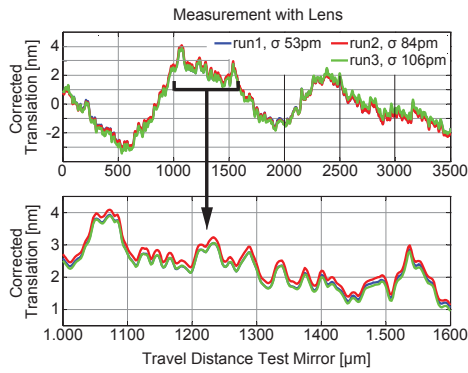


Fig. 7. Measurement results with focussed laser beam and therefore highly improved lateral resolution (top) and a detailed section of the measurement for better representation (bottom). The standard deviation σ for the different runs of each measurement are printed in the appendant legend.

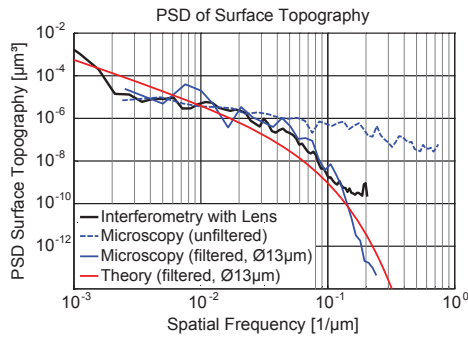


Fig. 8. PSD of the surface topography for both used experimental measurement methods (interferometry and interference microscopy) and the theoretical model.

beam with diameter d and the size of the (flat) test mirror is $D \gg d$. The spectra of the mirror surface $w(f)$ is $\approx r \cdot f^{-2}$ (resulting from a typical manufacturing / polishing process) with $r \approx 4.1 \cdot 10^{-10} \mu\text{m}$, determined from the experimental data. Under these assumptions, the path length errors m can be expressed with equation 4.

$$m(f) \approx w(f) \cdot h(f) = r \cdot f^{-2} \cdot h(f) \quad (4)$$

With

$$h(f) = e^{-\left(\frac{1}{2} \cdot \pi \cdot d \cdot f\right)^2} \quad (5)$$

as a "low-pass" filtering function that accounts for the effect of averaging of surface irregularities over the beam diameter. An additional contribution in the PSD due to the beam walk of the reference laser beam was investigated, but it has only an impact in spatial frequencies below $10^{-3} \mu\text{m}^{-1}$ that are not considered here.

Figure 8 shows the PSD of the interferometric measurement results with focussed laser beam, the corresponding unfiltered and filtered interference microscopy measurement results and the results of the theoretical model, parameterised with a beam diameter of $d = 13 \mu\text{m}$. The curve progression is similar for both experimental data as well as the theoretical data, even

the decrease of the curves due to the "low pass" filter effect of the laser beam shows good agreement.

V. CONCLUSION

The measurement results show surface induced path length errors with an amplitude of some nm, depending on the utilized laser beam diameter. That is considerably larger than the required pm scale of LISA, but their actual impact in the LISA measurement band is potentially small, considering the slow movement of the laser beam over the mirror surface in an annual cycle. Due to the high reproducibility of the measurement results demonstrated here, a calibration strategy is conceivable, that would allow to reject path length errors from IFP mirror movement in the telescope.

ACKNOWLEDGMENT

This work was funded by the German Aerospace Center DLR, using resources of the federal ministry for economics and technology under funding code 50 OQ 0701 "Untersuchungen zur Systemleistung alternativer Nutzlastkonzepte für LISA".

REFERENCES

- [1] ESA; LISA, Unveiling a Hidden Universe; Assessment Study Report, 2011;
- [2] ESA; NGO, Revealing a Hidden Universe: Opening a New Chapter of Discovery; Assessment Study Report, 2011;
- [3] Astrium GmbH; Assessment of a Next Generation Gravity Mission to Monitor the Variations of Earth's Gravity Field; Executive Summary, 2011;
- [4] M. Dehne, F. Guzman Cervantes, B. Sheard, G. Heinzel, K. Danzmann; Laser Interferometer for Spaceborne Mapping of the Earth's Gravity Field; Journal of Physics: Conference Series, 2009;
- [5] D. Weise, P. Marenaci, P. Weimer, H. R. Schulte, P. Gath, U. Johann; Alternative Opto-Mechanical Architectures for the LISA Instrument; Journal of Physics: Conference Series, 2009;
- [6] D. Weise, P. Marenaci, P. Weimer, M. Berger, H. R. Schulte, P. Gath, U. Johann; Opto-Mechanical Architecture of the LISA Instrument; Proceedings of the 7th ICSO, 2008;
- [7] D. Pantzer, J. Politch, L. Ek; Heterodyne Profiling Instrument for the Angstrom Region; Applied Optics, 1981;
- [8] G. E. Sommaergren; Optical Heterodyne Profilometry; Applied Optics, 1986;
- [9] T. Schuldt, M. Gohlke, D. Weise, U. Johann, A. Peters, C. Braxmaier; Picometer and Nanoradian Optical Heterodyne Interferometry for Translation and Tilt Metrology of the LISA Gravitational Reference Sensor; Classical and Quantum Gravity, 2009;
- [10] R. Spero; Optical Path Error from Beamwalk Across Irregular Mirror Surfaces; 1998;
- [11] D. Gerardi; Advanced Drag-Free Concepts for Future Space-Based Interferometers; PhD. Thesis (under submission), 2012;